Open Innovation for Phenotypic Drug Discovery: The PD^2 Assay Panel

JONATHAN A. LEE,[1] SHAOYOU CHU,[1*] FRANCIS S. WILLARD,[1*] KAREN L. COX,[1*] RACHELLE J. SELLS GALVIN,[1*] ROBERT B. PEERY,[1] SARAH E. OLIVER,[1] JENNIFER OLER,[1] TAMIKA D. MEREDITH,[1] STEVEN A. HEIDLER,[1] WENDY H. GOUGH,[1] SABA HUSAIN,[1] ALAN D. PALKOWITZ,[2] and CHRISTOPHER M. MOXHAM[1]

Phenotypic lead generation strategies seek to identify compounds that modulate complex, physiologically relevant systems, an approach that is complementary to traditional, target-directed strategies. Unlike gene-specific assays, phenotypic assays interrogate multiple molecular targets and signaling pathways in a target "agnostic" fashion, which may reveal novel functions for well-studied proteins and discover new pathways of therapeutic value. Significantly, existing compound libraries may not have sufficient chemical diversity to fully leverage a phenotypic strategy. To address this issue, Eli Lilly and Company launched the Phenotypic Drug Discovery Initiative (PD^2), a model of open innovation whereby external research groups can submit compounds for testing in a panel of Lilly phenotypic assays. This communication describes the statistical validation, operations, and initial screening results from the first PD^2 assay panel. Analysis of PD^2 submissions indicates that chemical diversity from open source collaborations complements internal sources. Screening results for the first 4691 compounds submitted to PD^2 have confirmed hit rates from 1.6% to 10%, with the majority of active compounds exhibiting acceptable potency and selectivity. Phenotypic lead generation strategies, in conjunction with novel chemical diversity obtained via open-source initiatives such as PD^2, may provide a means to identify compounds that modulate biology by novel mechanisms and expand the innovation potential of drug discovery. (*Journal of Biomolecular Screening* 2011;16:588-602)

Key words: open source, open innovation, PD^2, phenotypic drug discovery, lead generation

INTRODUCTION

Eli Lilly and Company is enhancing its classic, target-directed drug discovery (TDD) efforts with a lead discovery process in which compounds are tested in complex cell-based systems representing a more physiologically relevant context and assay environment. This phenotypic drug discovery (PDD) strategy shares roots with early, physiological drug discovery approaches but uses modern, multidisciplinary technologies. Such neoclassic PDD approaches can efficiently support screening, hit expansion, and structure-activity relationship (SAR) efforts[1,2] while simultaneously interrogating multiple, biologically relevant molecular targets and pathways. PDD therefore has the potential to discover compounds that modulate relevant biological processes in a target- and mechanism-agnostic fashion and has led to the discovery of novel targets involved in cell cycle,[3] cell migration,[4] and stem cell self-renewal.[5]

The PDD paradigm may expand the potential to identify high-quality drug candidate molecules. As a result, Lilly established a panel of assay modules composed of a phenotypic lead generation assay and relevant biochemical and cellular assays designed to define a compound's activity profile and potential for further drug optimization. To foster collaboration between industry and academia and to expand the available chemical diversity with which to screen, Lilly now provides access to these phenotypic assay modules to external investigators through its Phenotypic Drug Discovery initiative called PD^2 (https://pd2.lilly.com/pd2Web/).

This communication describes the statistical validation, operations, data analysis methods, and initial screening data related to the first five phenotypic screening assays available via PD^2. Each assay module represents therapeutic areas of strategic interest to Lilly, including metabolic diseases, neurological disorders, and oncology.

Insulin secretion. Although extensively studied, marketed small-molecule insulin secretagogues are glucose independent and lead to undesirable hypoglycemia in patients.[6] Glucose-dependent insulin secretagogues therefore offer a significant advantage over existing therapies; toward this end, we describe

[1]Department of Quantitative and Structural Biology, Lilly Research Laboratories, Eli Lilly and Company, Indianapolis, Indiana.
[2]Discovery Chemistry Research and Technologies, Lilly Research Laboratories, Eli Lilly and Company, Indianapolis, Indiana.

[*]These authors contributed equally to the work.

Received Nov 16, 2010. Accepted for publication Dec 15, 2010.

Supplementary material for this article is available on the *Journal of Biomolecular Screening* Web site at http://jbx.sagepub.com/supplemental.

Journal of Biomolecular Screening 16(6); 2011
DOI: 10.1177/1087057111405379

the first medium-throughput screen (MTS)–ready assay measuring glucose-dependent insulin secretion from pancreatic INS-1E cells.

Osteoporosis. The canonical Wnt pathway is highly validated in bone development.[7,8] The Wnt-dependent differentiation of C2C12, a multilineage potential cell line, into an osteoblast-like phenotype provides a model of osteogenesis amenable to MTS.

Alzheimer disease (AD). Allelic variation in apolipoprotein E (ApoE) has been identified as an important genetic risk factor for the development of sporadic AD[9,10]; several lines of evidence suggest that secreted ApoE forms high-affinity extracellular complexes with β-amyloid peptide (Aβ), a major constituent of amyloid plaques in brains of AD patients, and facilitates the proteolytic degradation and or efflux of Aβ from the AD brain. Statistical validation of ApoE secretion from the astrocyte cell line, CCF-STTG1, enables the operation of a phenotypic assay for novel ApoE secretagogues.

Cell division. Cell cycle arrest is a long-established mechanism for the development of oncology therapeutics. The validated, high-content DNA content assay described here provides a means to identify compounds that arrest cell cycle in G2 or M; identification of such agents that used tubulin-independent mechanisms may be a class of cell cycle inhibitor with diminished neurotoxicity.[11]

Angiogenesis. Tumor progression requires the development of a blood vessel network to support continued growth[12]; current antiangiogenesis agents inhibit the tyrosine kinase receptor for vascular endothelial growth factor (VEGF),[13] the dominant proangiogenic factor.[14] Validation of an angiogenesis assay using co-culture of endothelial colony-forming cells (ECFCs) and human adipose–derived stem cells (ADSCs) captures, in part, the biological complexity of neovascularization and enables a PDD assay to identify compounds that inhibit angiogenesis by novel mechanisms.

The results from testing the first several thousand PD^2 compounds indicate that a large percentage (2–10%) of these structurally distinct molecules demonstrate confirmed activity in a PD^2 assay and display median potencies in the low micromolar range. Significantly, the majority of confirmed PD^2 actives (70%) modulate only a single PDD assay. The implications of these observations to biologically relevant chemical diversity, PDD, and the identification of novel therapeutic mechanisms of action are discussed.

MATERIALS AND METHODS

Detailed materials and methods are provided in the **supplementary information** online.

Methods common to assays

All cell growth and cell-based assay incubations were conducted at 37 °C, in a humidified incubator at 5% CO_2 unless otherwise noted. Percentage stimulation and percentage inhibition were calculated by equation 1 and equation 2, respectively, using the maximum (Max) and minimum (Min) response conditions for each assay as described in the **supplementary information**.

$$\textit{Equation 1: Stimulation}\ (\%) = \frac{Signal - Min}{Max - Min} \times 100$$

$$\textit{Equation 2: Inhibition}\ (\%) = 1 - \left(\frac{Signal - Min}{Max - Min}\right) \times 100$$

The EC_{50} or IC_{50} of test compounds was determined by fitting the calculated percentage activation or inhibition values using a standard four-parameter logistic and nonlinear regression analysis.

All assays were validated for plate uniformity (three plates each of high, mid, and low signal per day for 3 days) and potency reproducibility (>20 compounds of varying potency tested in two independent experiments) in accordance with the published Eli Lilly–NIH Chemical Genomics Center guidelines for assay enablement and statistical validation (http://www.ncgc.nih.gov/guidance/index.html).

Insulin secretion assay

INS-1E cells seeded in 384-well plates were treated with compounds at the indicated concentration in either high (5 mM glucose and 1.5 uM 3-isobutyl-1-methylxanthine [IBMX]) or low (0.1 mM glucose and 1.5 uM IBMX) glucose conditions for 1 h. Secreted insulin (ng/mL) was determined by an Insulin AlphaLISA™ kit using purified human insulin (Lilly Research Laboratories) as a standard.

ApoE secretion assay

CCF-STTG cells seeded in 384-well plates were treated with compounds at the indicated concentration in assay media for 70 h. Secreted ApoE was determined by an AlphaLISA™ kit using purified ApoE (Biodesign) as a standard.

Wnt pathway assay

Wnt3A conditioned media (CM) were prepared as described.[15] C2C12 cells seeded in 384-well plates were treated Wnt3A, bone morphogenetic protein 4, and compounds at the indicated concentration for either 24 h or 48 h before measuring β-catenin located in cell nuclei or cell-associated alkaline phosphatase (ALP) activity, respectively.

Table 1. Statistical Validation Results of PDD Assays: Z′ and Minimum Significant Ratio (MSR)

Assay	*Z′*	*MSR*
ApoE secretion	0.48	3.4
Angiogenesis	0.42	2.2
G2/M arrest		
Cyclin B + pH3	0.63	2.1
>2N	0.63	2.7
2N	0.63	2.5
4N	0.59	2.2
DNA condensation	0.7	3.3
Insulin secretion		
0.1 mM glucose	0.73	2.4
5.0 mM glucose	0.62	2.8
Wnt pathway		
β-catenin	0.64	2.7
ALP activity	0.55	1.7

From assay validation studies. The Z′ is the average over 3 days of plate uniformity testing. The MSR is calculated from 2 days of compound potency testing using 20 to 30 compounds in each assay.

Angiogenesis assay

Co-cultures of human clonal ECFCs with human adipose ADSCs seeded in 384-well plates were treated with VEGF and compounds at the indicated concentration for 96 h prior to fixation, staining, and measuring of endothelial tube area and cell nuclei.

G2M cell cycle assay

Human cervical tumor (HeLa) cells seeded in 384-well plates were treated with compounds at the indicated concentration for 24 h prior to fixation, staining, and measuring DNA content, DNA condensation, and cellular CyclinB + phosphorylated histone H3 (pH3).

RESULTS

Statistical validation of assays

To ensure operational robustness, in vitro assays used to make critical path decisions require statistical validation. The Z′ score is a metric for interplate and interexperimental variation of signal window.[16,17] The statistical validation results for the five phenotypic assays are summarized in **Table 1**. Average Z′ values over multiple days and runs range from 0.42 to 0.73 (**Table 1**); column- and row-wise analysis of the plate uniformity data demonstrated no evidence of edge effects (not shown). The reproducibility of potency determinations is evaluated by experimentally determining the assay minimum significant ratio (MSR); if two compounds have a within-run potency ratio >MSR, then the potency differences between the compounds are statistically significant.[18] The MSR values for each phenotypic assay channel ranged from 1.7 to 3.4 (**Table 1**). Taken together, the plate uniformity and MSR analysis indicate that each phenotypic assay is suitable for MTS and provides reliable potency measurements for lead optimization using singlet determinations.

Insulin secretion

The rat insulinoma cell line INS-1E exhibits many of the phenotypic characteristics of pancreatic β cells, including glucose-stimulated insulin secretion, and is thus a useful model to screen for compounds that cause glucose-dependent insulin secretion.[19] Insulin release using the 384-well INS-1E assay is stimulated by glucose from 10- to 30-fold in a saturable manner and is potentiated by cAMP elevation with IBMX (**Fig. 1A**). The glucose-stimulated insulin release was highly cooperative, with EC_{50} values of 7 to 8 mM (**Fig. 1A**), consistent with the pharmacology of glucose sensing in β cells.[20]

Known insulin secretagogues, the sulfonylurea glyburide (glibenclamide), the glucokinase activator LY2121260,[21] the protein kinase C activator phorbol 12-myristate 13-acetate (PMA), and the imidazoline LY374284[22] were tested in the INS1-E phenotypic assay at 5 mM and 0.1 mM glucose concentrations (**Fig. 1B**, **C**). PMA was observed to be a highly potent and efficacious insulin secretion agent at both 0.1 mM and 5 mM glucose. Glyburide, a drug in clinical use, was observed to be a highly potent insulin secretagogue with efficacy at 5 mM glucose and low but detectable efficacy at 0.1 mM glucose (**Fig. 1B**, **C**). This is consistent with glyburide's known action and its propensity to promote hypoglycemia in patients,[6] an undesirable trait for future therapeutic compounds. In contrast, the glucokinase activator LY2121260 and the imidazoline LY374284 were highly efficacious insulin secretagogues at 5 mM glucose yet inactive at 0.1 mM glucose, consistent with their known pharmacology and lack of hypoglycemic effects,[21,22] an activity profile that is desirable for therapeutic insulin secretagogue agents. All four reference compounds exhibited potencies and efficacies consistent with those previously described in insulinoma cells or rodent islets[21,23,24]; however, it must be noted that some known β-cell secretagogues such as glucagon-like peptide-1, gastric inhibitory polypeptide, and oxotremorine are inactive in this assay. Taken together, these results indicate that the INS-1E insulin secretion assay can reliably detect and differentiate between insulin secretagogue with different mechanisms of action.

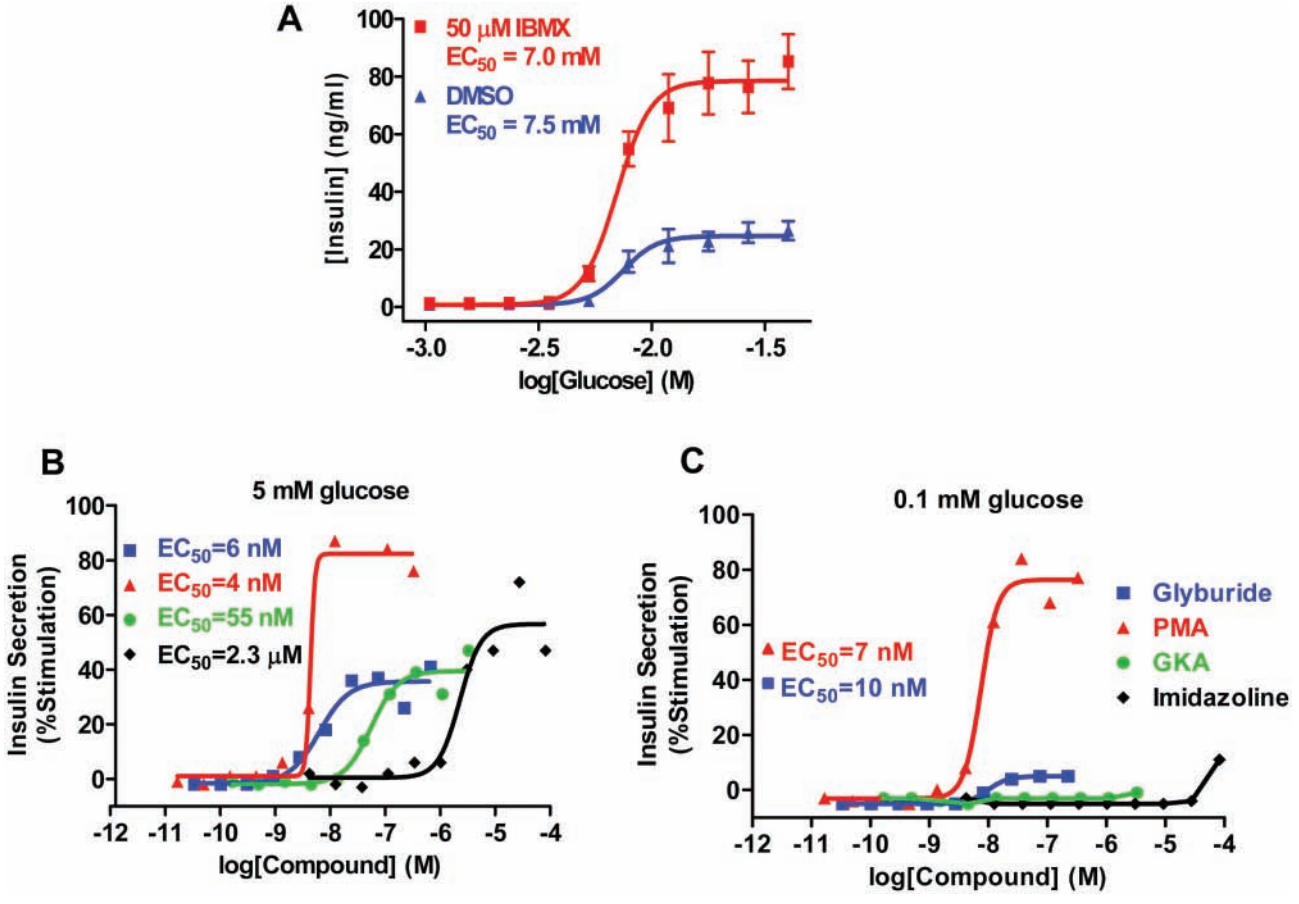

FIG. 1. Development of a glucose-stimulated insulin secretion (GSIS) assay for medium-throughput screening (MTS). (**A**) The potency of GSIS by INS-1E cells was determined at the indicated glucose concentration in the absence or presence of IBMX (50 μM). (**B, C**) The indicated compounds were tested in concentration response format for their ability to cause insulin secretion in INS-1E cells at 5 mM (**B**) and 0.1 mM (**C**) glucose concentrations as described in the supplement to the Materials and Methods section. GKA and imidazoline are LY2121260 and LY374284, respectively.

ApoE Secretion

The human astrocytoma cell line CCF-STTG1 constitutively secretes ApoE and forms lipoprotein complexes.[25] Treatment of CCF-STTG1 cells with a liver X receptor (LXR)–specific agonist, T-O901317,[26] results in a concentration-dependent increase in ApoE secretion with an EC_{50} of 8.6 nM (**Fig. 2A**), which is in good agreement with reported affinity for LXR-β[26] and a previous ApoE secretion study.[27] Test compound effects on nonspecific leakage of cytoplasmic proteins were monitored by release of lactate dehydrogenase (LDH) into the media. T-O901317 increased LDH release at concentrations 1000-fold greater than the EC_{50} for induction of ApoE secretion (**Fig. 2A**, **B**). These data confirm that CCF-STTG1 is a suitable cellular model for ApoE secretion from astrocytes.[27] A statistically validated ApoE secretion assay (**Table 1**) in conjunction with a counterscreen for nonspecific CCF-STTG1 cell permeability (**Fig. 2B**) and an LXR biochemical assay provide an effective means to identify compounds that stimulate ApoE secretion through non-LXR mechanisms.

Osteoblast differentiation, Wnt pathway

In C2C12 cells not treated with a glycogen synthase kinase-3 (GSK3) inhibitor, the majority of β-catenin is located within the adherens junctions between clusters of C2C12 cells; activation of the Wnt pathway by GSK inhibition results in β-catenin accumulation and translocation into the nucleus (**Fig. 3A-B**). Activation of the Wnt pathway in C2C12 cells also results in the induction of cellular ALP activity, a marker for osteoblast differentiation[28] (**Fig. 3C**, **D**).

The Wnt pathway assay measures β-catenin localized within cell nuclei and cell-associated ALP activity at optimal time points

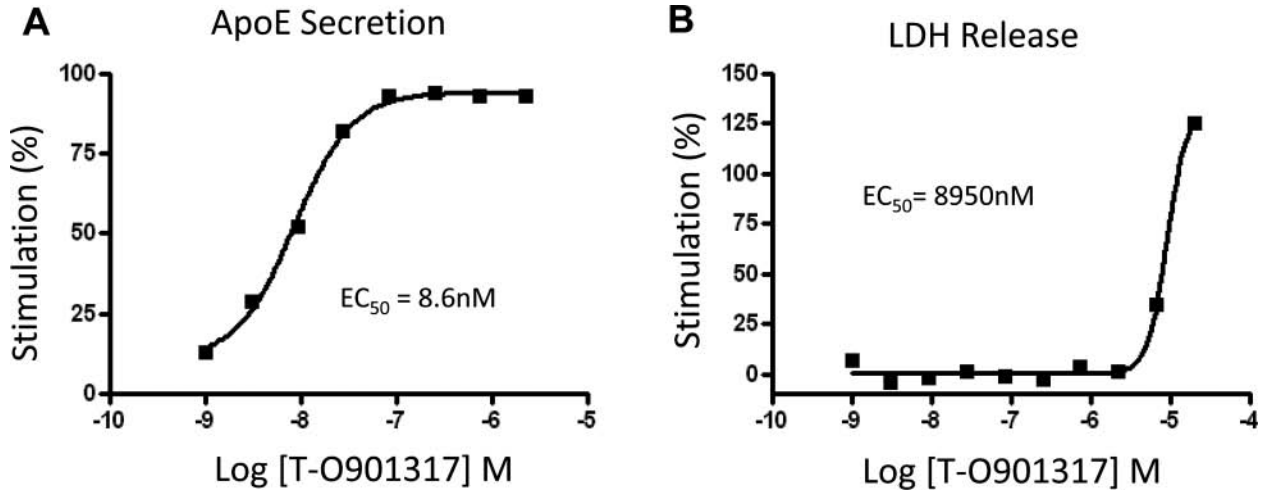

FIG. 2. Liver X receptor (LXR) agonist T-O901317 selectively enhances apolipoprotein E (ApoE) secretion from CCF-STTG1 cells. Cells were treated with the indicated concentrations of T-O901317, and the release of cellular ApoE (**A**) and lactate dehydrogenase (LDH; **B**) was measured separately, as described in the supplement to the Materials and Methods section.

of 24 and 48 h, respectively. Treatment with CM from L cells expressing Wnt3A resulted in β-catenin translocation in a dose-dependent manner (**Fig. S1**). Because the primary goal of the Wnt pathway screen is to identify molecules that either induce or potentiate β-catenin translocation and induce osteoblast differentiation, the validated assay included Wnt3A CM to activate β-catenin translocation to 20% of maximal Wnt3A activity (**Table 1**). Wnt pathway activation by a GSK3 inhibitor shows a dose-dependent increase in nuclear β-catenin and ALP activity; the average EC_{50} values for β-catenin translocation and stimulation of ALP activity were 38 nM and 8 nM, respectively (**Fig. 3E**, **F**), which are similar to the 3-nM value reported for inhibition of cellular Tau phosphorylation.[29] It is important to note that although a GSK3 inhibitor serves as a convenient positive control, the resulting β-catenin responses are superphysiological, with maximum efficacies 3- to 4-fold higher than the corresponding value for Wnt3A CM. Validation of this multiparametric Wnt pathway assay (**Table 1**) provides a means to identify compounds that induce an osteoblast-like lineage in a β-cateninen dependent manner.

Angiogenesis

ECFCs form tubelike structures that express the endothelial marker CD31 when co-cultured on an ADSC feeder layer (**Fig. S2A**). Three outputs from the Cellomics Tube Formation Bioapplication—total tube area, mean tube node count, and mean tube length width ratio—were compared in a time course experiment; total area was the most sensitive measure of tube formation (**Fig. S2B**) and was used for assay validation (**Table 1**) and subsequent studies. The multiplexed measurement of cell nuclei area in the same sample provides an important measure of relative cytotoxicity (**Fig. 4A**). Sutent, a marketed antiangiogenic drug that inhibits VEGFR2 and other receptor tyrosine kinases,[13] inhibits co-culture tube formation in a dose-dependent manner (**Fig. 4A**). Quantitative dose-response curves of CD31 tube formation and cellular nuclei indicate that Sutent inhibits angiogenesis with an IC_{50} value of 16 nM without exhibiting overt cytotoxicity (**Fig. 4B**). In contrast, compounds that decrease tube formation and cell nuclei area are probably inhibiting angiogenesis through undesirable cytotoxic mechanisms (**Fig. 4B**). The multiplexed measurement of CD31 tube area and cytotoxicity thus provides a means to readily differentiate potentially interesting active compounds from false-positives in the angiogenesis screen.

Cell cycle inhibition, G2/M arrest

High-content cellular imaging is a powerful tool to analyze cell cycle and associated biological events such as apoptosis or reorganization of cellular tubulin.[30–32] **Figure 5A** shows the number of cells as a function of propidium iodide (PI) fluorescence intensity, a measure of cellular DNA; the resulting distribution describes the DNA content for the population of sampled cells. Major peaks corresponding to diploid (2N) and tetraploid (4N) cell populations correspond to cells in G1 and G2 and/or mitosis (M) cell cycle stages, respectively (**Fig. 5A**). Cells with PI fluorescence intensity between 2N and 4N correspond to a population of cells that are replicating DNA (S phase). In addition to DNA content, the assay measures levels of cellular CyclinB and pH3, biomarkers for the G2 and M phases, respectively (**Fig. 5A**, **B**).[1] Finally, information on the condensation state of cellular DNA provides an independent measure of M-phase cells or other cellular processes that lead to DNA

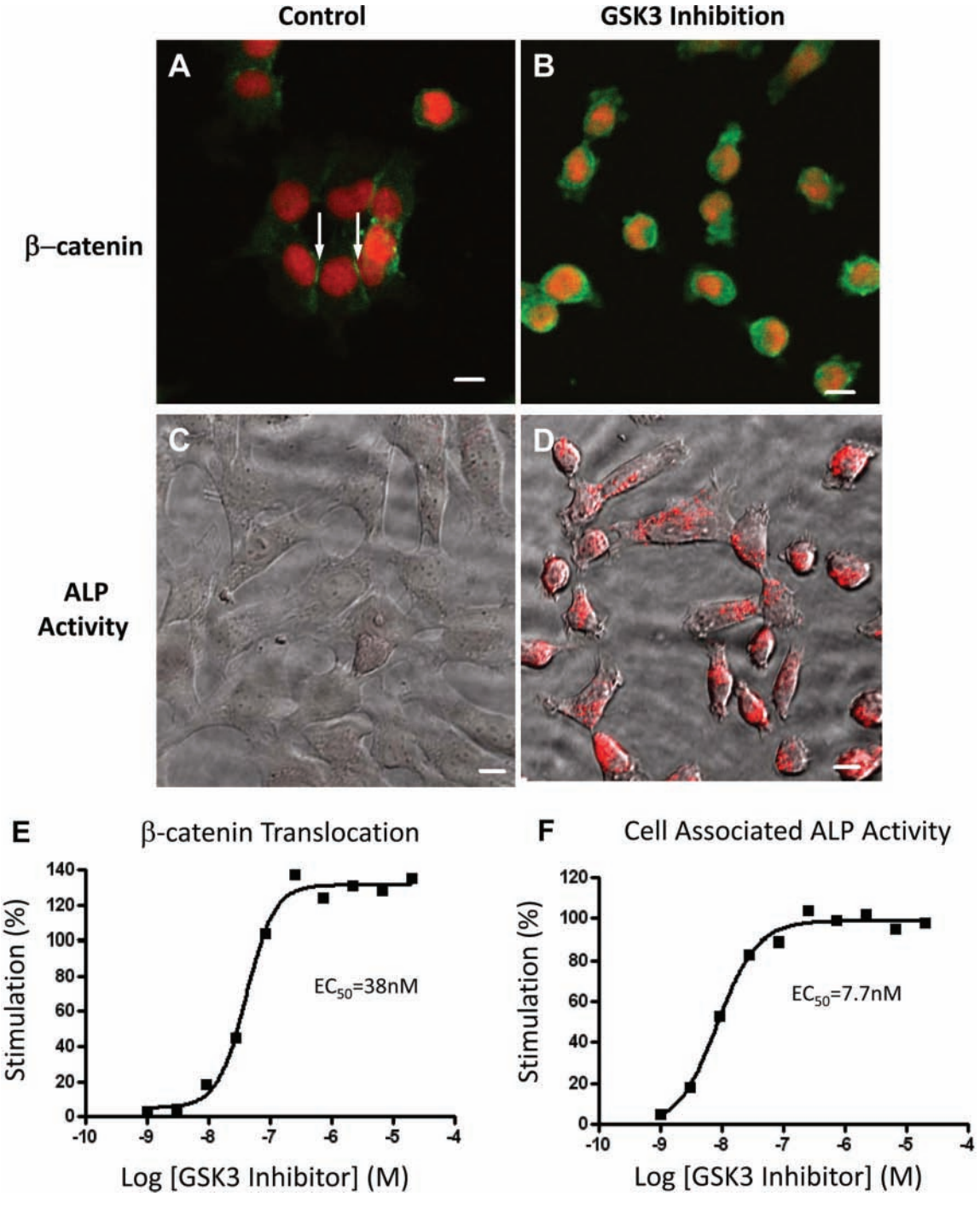

FIG. 3. Glycogen synthase kinase-3 (GSK3)–β inhibition causes β-catenin translocation and induction of alkaline phosphatase activity in C2C12 cells. (**A, B**) Staining of β-catenin (green) and nuclei (red). β-catenin in unstimulated C2C12 cells is predominantly located in the adhesion junctions between clusters of C2C12 cells (**A**, arrows). Following stimulation of the Wnt pathway by GSK3-β inhibitor treatment, β-catenin is located in the nucleus and cytosol (**B**). (**C, D**) Overlay of transmitted light and fluorescence images. Cellular alkaline phosphatase (ALP) activity (red) increases optimally after a 48-h treatment with a GSK3-β inhibitor (**D**); untreated cells display very low cellular ALP activity (**C**). Bars = 10 uM. (**E**) GSK3-β inhibitor increases β-catenin translocation and cellular ALP activity (**F**) in C2C12 cells. The assay contained bone morphogenetic protein 4, an EC_{20} of Wnt3A conditioned media to provide a basal Wnt pathway tone; the pathway was further stimulated by addition of indicated concentration of GSK3-β inhibitor. β-catenin translocation and cell-associated ALP activity were measured by laser scanning cytometry, as described in the supplement to the Materials and Methods section.

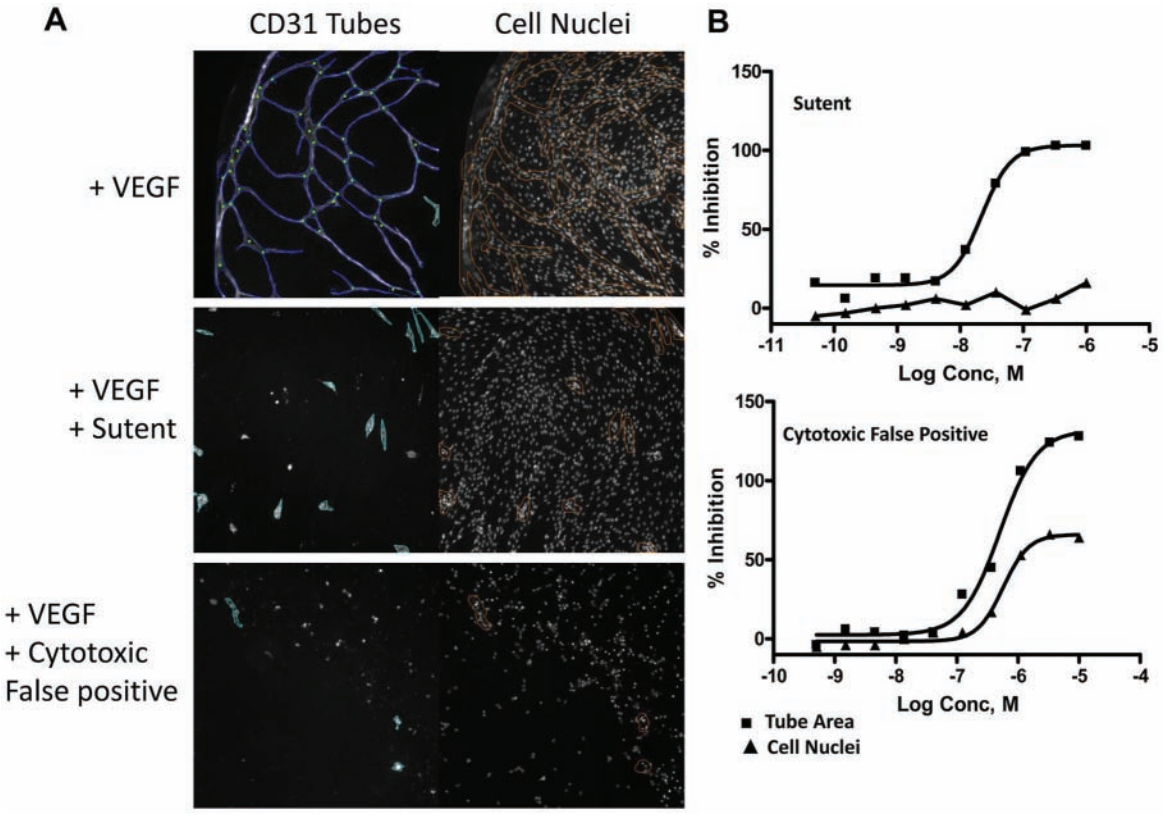

FIG. 4. Inhibition of endothelial tube formation. (**A**) CD31-positive endothelial tube-like structures (**left**) and nuclei (**right**) 96 h following addition of vascular endothelial growth factor (VEGF), VEGF + Sutent, or VEGF + cytotoxic compound. (**B**) Multiplexed inhibition of total CD31 tube and total nuclei area. Sutent or a cytotoxic compound was incubated with the endothelial colony-forming cell (ECFC)–human adipose–derived stem cell (ADSC) co-culture for 96 h at the indicated concentrations.

condensation such as apoptosis.[33] Nocodazole treatment arrests the cell cycle in the M phase[34] and leads to decreased 2N and increased 4N, cyclinB-pH3, and DNA condensation (**Fig. 5A**, **B**). This multiplexed cell cycle assay is statistically validated for plate uniformity and potency reproducibility (**Table 1**); as a result, compound dose-response curves provide high-quality data and reproducible potency values using singlet determinations (**Fig. 5C**).

Simultaneous measurement of DNA content, DNA condensation, and cyclin B-pH3 status following compound treatment results in a multiplexed cell cycle activity profile that differentiates various cell cycle phases such as G2 and M following doxorubicin and nocodazole treatment, respectively.[1] Clustering algorithms segregate multiplexed compound potency activity profiles into phenotypic classes represented by various grids within the self-organizing map (**Fig. 5D**) where each grid phenotype is defined by the potency of a compound to modulate various cell cycle parameters. Profiles C1R1-2 and C2R1-3 correspond to compounds that modulate CycB/pH3, DNA content, and DNA condensation with high and equal potency, an activity profile that is consistent with a block in mitosis. Internal Lilly screening identified compounds that modulate CycB/pH3 and all DNA content channels with high and equal potency but had greatly reduced or undetectable effect on DNA condensation (data not shown); this assay profile is consistent with a G2 phenotype.[1] Compounds with profiles C3R1, C3R4, and C4R3 (**Fig. 5D**) induce DNA condensation without potent modulation of DNA content; this cellular phenotype is consistent with the induction of apoptosis. Interestingly, unknown cellular phenotypes corresponding to potent modulation of DNA content without detectable activation of CycB-pH3 (**Fig. 5D**, C1R4) and potent activation of CycB-pH3 in the absence of potent DNA content modulation (**Fig. 5D**, C4R4) are observed. PD^2 compounds exhibiting either a G2 or M cellular phenotype are of potential interest as oncology agents.

PD^2 collaboration metrics

As of December 2010, a total of 195 institutions were affiliated with PD^2. Following the official opening of the PD^2 Web site in June 2009, the number of registered account users has steadily increased to more than 290 investigators. Analysis of global demographic data indicates that PD^2 collaborators are affiliated with academia (61%), biotech (32%), and research

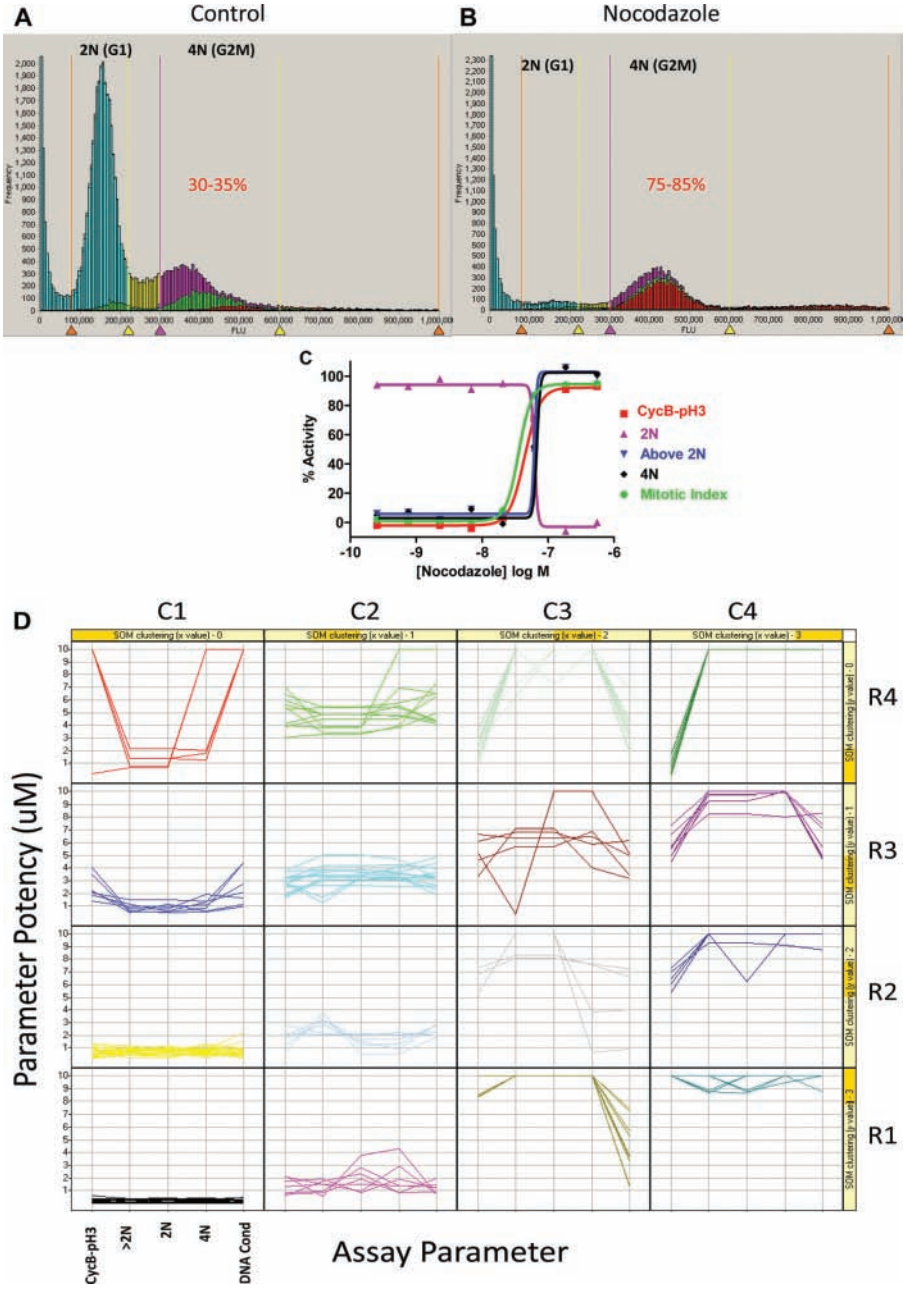

FIG. 5. Multiplexed cell cycle assay monitoring DNA content, cyclinB-pH3 levels, and DNA condensation in HeLa cells. (**A**) The DNA content histogram of untreated cells; 2N (G1) and 4N (G2M) cell populations are indicated. (**B**) Nocodazole treatment induces a G2M arrest, with the 4N cell population increasing from 35% to 85%. Multiplexed endpoints define different cell populations: 2N DNA content (blue), 4N DNA content (magenta), 2N-4N DNA content (yellow), condensed DNA (red), and CyclinB-pH3 (green). (**C**) Dose response of nocodazole-induced G2/M cell cycle arrest. HeLa cells were treated with nocodazole at the indicated concentrations, and multiplexed cell cycle parameters were measured as described in the supplement to the Materials and Methods section. (**D**) Self-organizing map (SOM) of G2M assay actives: PD^2 single-point screen hits were confirmed in 10-point dose-response mode and by determination of potencies for CycB-pH3, DNA content, and DNA condensation as described in the supplement to the Materials and Methods section. Clustering of the resulting five compound potency data sets by SOM analysis indicates the existence of several phenotypic classes. Each assay profile is a grid within the SOM, which consists of the EC_{50} or IC_{50} of the assay parameter versus the five assay parameters, CycB-pH3, >2N, 2N, 4N, and DNA condensation, respectively. Each activity profile is designated by a row (R1–4) and column (C1–4). C1R1-2 and C2R1-3 correspond to compounds inducing a mitotic block. Compounds in C3R1, C3R4, and C4R3 lead to an increase in DNA condensation without affecting DNA synthesis and may be inducing apoptosis. Compounds in C1R4 and C4R4 correspond to unknown phenotypes related to changes in DNA content without increasing CycB-pH3 levels and activation of CycB-pH3 in the absence of alterations of DNA content, respectively.

institutes (7%), located in the United States (55%), Europe (28%), and Asia (9%), with the remaining collaborators located in the Americas, Pacific, and Middle East. Similarly, the number of compounds submitted to PD^2 has grown steadily over time. At the end of Q4 2010, a total of 29 760 compounds have been submitted for cheminformatics analysis for structural novelty, and 17 835 compounds were accepted to the PD^2 Initiative. This suggests that 60% of the compounds submitted for analysis of structural novelty are less than 85% similar (Tanimoto coefficient <0.85) to known drugs, previously submitted PD^2 compounds, and molecules registered in the Lilly collection (https://pd2.lilly.com/pd2Web/DefaultMenuItems/others/PD2_Structure_Evaluation_Details.pdf) and are unlikely to possess similar molecular mechanisms.[35]

As of September 2010, 4691 compounds have been tested in the PD^2 modules (**Figs. 1**–**5**). Dose-response follow-up of single-point screen actives indicates that 1.6% to 10% of the PD^2 compounds tested have confirmed activity in at least one of the phenotypic screens. These confirmed actives demonstrated potencies with median IC_{50} or EC_{50} values ranging from 1.7 uM (G2M) to 4.3 uM (insulin), with high-potency compounds identified in the Angio, Wnt, and G2M modules (EC_{50} or IC_{50}values <10 nM) and intermediate potency compounds in the ApoE and insulin modules (EC_{50} 100 and 330 nM, respectively).

Specificity of biological action is an important metric related to the potential quality of a therapeutic compound and screen active. **Figure 6A** is a summary of the confirmed activity of the PD^2 compounds as of September 2010. Hierarchical clustering of the pEC_{50} or pIC_{50} values for each phenotypic module provides information on the selectivity of confirmed actives across the five PD^2 modules. The majority (70%) of compounds are selective compounds and modulate only one PD^2 module (**Fig. 6A**), with 22% and ~8% of the compounds active in two and three modules, respectively (**Fig. 6A**). Although the compounds active in three PD^2 modules had higher average potencies, the overall data indicate that promiscuous biological activity does not appear to be prevalent (**Fig. 6A**). Although speculative, it may be possible that the activity of compounds across various PD^2 modules provides information on the similarities and differences of the underlying signaling pathways contributing to each phenotype as suggested by the expected quantitative correlation between the G2M arrest and inhibition of angiogenesis[36] for a subset of the angiogenesis PD^2 confirmed actives (**Fig. 6B**).

Early phenotypic characterization also provides a means to identify active molecules with higher therapeutic potential. **Figure 6C** shows the EC_{50} value for insulin secretion at low glucose, an undesirable activity, versus the EC_{50} value for insulin secretion at high glucose, a desirable activity. To date, only 8% of the confirmed actives at high glucose demonstrate activity at low glucose, suggesting that compounds derived from these actives will stimulate insulin secretion in a glucose-dependent fashion and are less likely to induce hypoglycemia.[21,22] Multiplexed determination of endothelial tube inhibition and nuclear area, a relative measure of cell toxicity, indicates that more than 80% of the confirmed antiangiogenic actives are working through noncytotoxicity mechanisms (**Fig. 6D**), a desirable trait. Parallel characterization of the Wnt pathway actives through nuclear localization of β-catenin and induction of the osteoblast marker, cellular ALP activity,[28] indicates that more than 70% of confirmed actives induce ALP activity and β-catenin translocation with similar EC_{50} values, suggesting a common mechanism (**Fig. 6E**) and providing a rationale to remove other compounds that may use other mechanisms of action.

DISCUSSION

Lilly Research Laboratories is using phenotypic assays to chemically interrogate complex biological systems composed of multiple or unknown biochemical components/pathways. Neoclassic PDD approaches complement gene-specific TDD strategies and thus may expand the potential to discover novel and effective medicines. Phenotypic assays, when appropriately enabled and statistically validated, have the testing capacity and quantitative reproducibility to efficiently support screening, hit expansion, and SAR efforts[1] (**Table 1**; **Figs. 1**–**5**), a frequent concern regarding the use of complex cell-based systems for drug discovery.

Much of the chemical diversity within pharmaceutical compound collections is derived from projects that sought to identify competitive inhibitors for kinases, G-protein coupled receptors (GPCRs), ion channels, nuclear hormone receptors, and enzymes. This raises the question of whether the pharmaceutical industry's chemical diversity is sufficient to fully leverage a target agnostic approach such as PDD. Recognizing this potential limitation, Eli Lilly and Company launched PD^2, an open-source initiative in which Lilly tests novel compounds from academic and biotech organizations free of charge while allowing the Lilly collaborator to retain data and full intellectual property rights with the hope of establishing drug discovery research collaborations. Information about this program can be found at https://pd2.lilly.com/pd2Web/, with detailed instructions on how principal investigators and research institutes can participate in PD^2. The PD^2 Web site also provides an overview of the current phenotypic assay modules, which includes the phenotypic screen and all cell-based and biochemical follow-up assays necessary to provide an initial evaluation of the submitted compounds. To meet the collaborative transparency required in open-source research efforts, this article provides experimental details on the operation, statistical validation, data analysis, and initial screening results associated with the first phenotypic assays of PD^2.

Diabetes: insulin secretion

Type 2 diabetes is a significant unmet medical need, with an estimated >7% of the U.S. population suffering from this condition. Type 2 diabetes is characterized by both insulin resistance

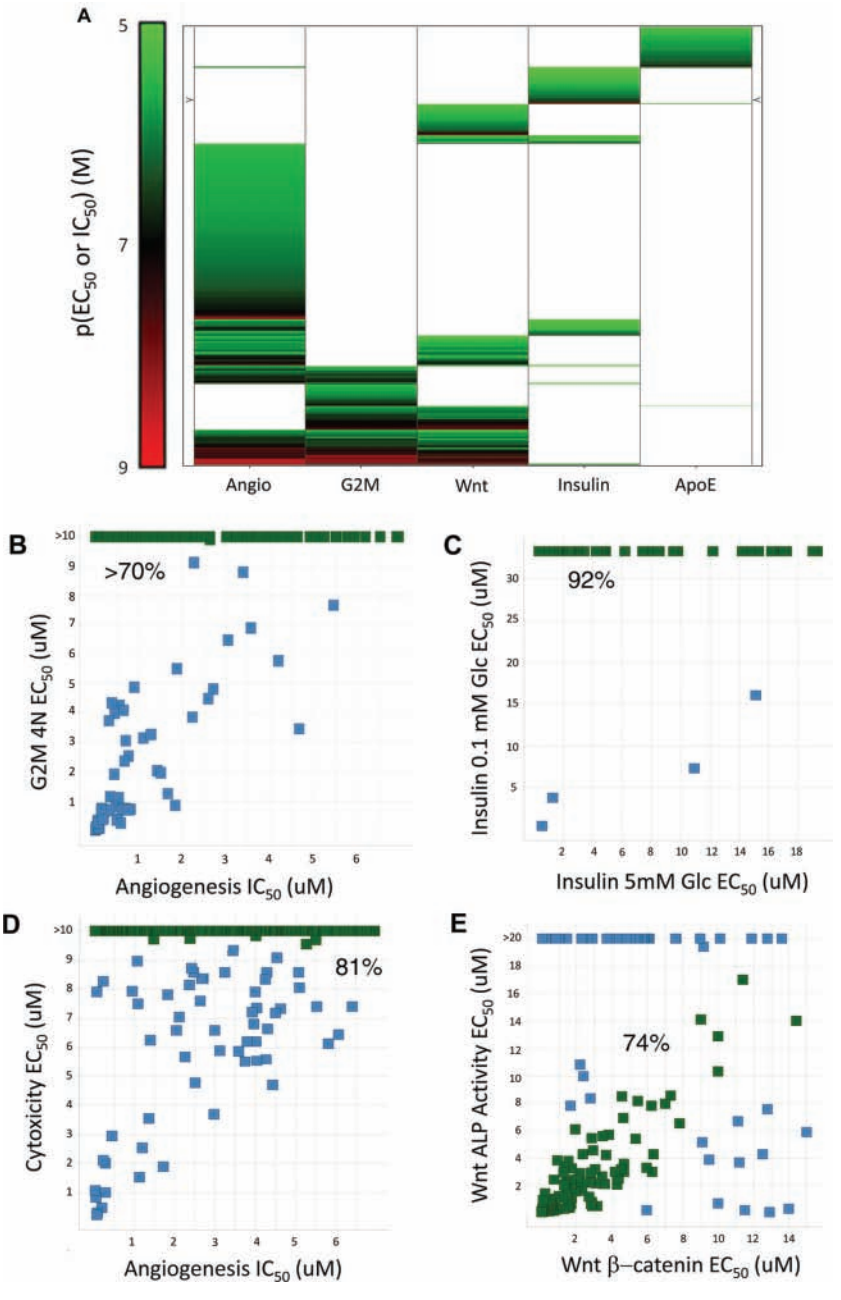

FIG. 6. Biological specificity of PD^2 compounds. (**A**) Hierarchical clustering of confirmed PD^2 actives. Compound activities in the indicated phenotypic assays were expressed as pIC_{50} or pEC_{50} (Molar) and then clustered using Spotfire. pEC_{50} or pIC_{50} values corresponding to 9 (red), 7 (black), and 5 (green) are indicated, as well as no measurable compound activity (white). (**B**) 4N activity in the G2M assay versus antiangiogenesis activity. Compounds inhibiting angiogenesis by blocking cell cycle, an undesirable mechanism, are indicated (blue); compounds inhibiting angiogenesis by non–cell cycle mechanisms, a desirable phenotype (green). (**C**) Insulin secretagogue activity at 0.1 mM glucose versus insulin secretagogue activity at 5.0 mM glucose. Compounds stimulating insulin secretion with similar potencies at high and low glucose, an undesirable mechanism, are indicated (blue); compounds stimulating insulin secretion in a glucose-dependent manner, a desirable mechanism (green). (**D**) Cytotoxicity versus antiangiogenesis activity. Compounds inhibiting angiogenesis by increasing cytotoxicity, an undesirable mechanism, are indicated (blue); compounds inhibiting angiogenesis without significant cytotoxicity, a desirable mechanism (green). (**E**) Activation of cellular alkaline phosphatase (ALP) activity versus β-catenin translocation. Compounds that disproportionally affect either cellular ALP activity or β-catenin translocation activity, an undesirable mechanism, are indicated (blue); compounds that proportionally enhance ALP activity and β-catenin translocation, a desirable mechanism (green). The percentage compounds having a desirable phenotypic profile are indicated for each PD^2 module.

and insufficient insulin secretion from the pancreatic β-cell. The pancreatic β-cell has a glucose-sensing mechanism to facilitate glucose-stimulated insulin secretion (GSIS) by secretagogues such as incretins, amino acids, and fatty acids. K^+_{ATP} channel modulators (sulfonylureas and glinides) remain the sole class of Food and Drug Administration–approved small-molecule insulin secretagogue agents that directly act on pancreatic β-cells.[6] These compounds are glucose-independent insulin secretagogues and thus have been associated with hypoglycemic events. Other small-molecule β-cell secretagogues in clinical development represent a limited number of molecular targets encompassing metabolic regulators such as glucokinase and a small number of GPCRs.[20,37] Despite more than a half-century of substantial effort from both academia and industry, a limited number of molecular targets that are tractable for small-molecule discovery have been associated with glucose-dependent insulin secretion.

The rat insulinoma cell line INS-1E exhibits GSIS and is thus a useful model to screen for compounds that are glucose-dependent insulin secretagogues. Reference molecules including a sulfonylurea, an imidazoline, and a glucokinase activator demonstrated appropriate glucose-dependent pharmacology for insulin secretion in INS-1E cells (**Fig. 1**). This is the first report of an assay for glucose-dependent insulin secretion that is amenable for MTS in a 384-well format. A prior study demonstrated that insulin release could be measured in INS-1E 832/13 cells using a 96-well format with triplicate data points,[38] making the assay system unsuitable for an MTS screening campaign. In contrast, our assay was capable of reproducibly detecting small-molecule insulin secretagogues over a wide range of potencies and efficacies. Compounds with different mechanisms of action were observed to give consistently distinct efficacies for insulin secretion. For instance, glyburide was moderately efficacious (mean = 40%, SEM = 2, $n = 67$), while PMA was highly efficacious (mean = 82%, SEM = 7, $n = 60$) relative to a maximal concentration of glucose. This assay, therefore, provides the capability to perform SAR quality analysis on both the potency and efficacy of molecules for lead optimization. The diabetes phenotypic module seeks to identify compounds that will enhance GSIS by novel mechanisms.

Alzheimer Disease: ApoE secretion

AD is a progressive degenerative dementia that usually begins with memory impairment and progresses to involve a severe loss of multiple areas of cognitive function. The ε4 allele of the ApoE gene was identified as an important genetic risk factor for the development of sporadic, late-onset AD.[9,10] Individuals who inherit one or two copies of the ApoE4 allele develop AD earlier and have a 2- and 10-fold risk, respectively, of developing the disease.[39] Consistent with the increased AD risk associated with the apoE4 allele, models using transgenic mice expressing human amyloid precursor protein (APP) and human ApoE4 have 10-fold higher expression of fibrillar (thioflavin-S-positive) Aβ and a twofold to threefold lower dendritic spine density in the dentate gyrus than APP transgenic mice expressing ApoE3.[40,41] Finally, the ApoE allelic differences in adult-onset AD also correspond with the ability of the various ApoE isoforms to facilitate the proteolysis of soluble Aβ within the brain[42] and mediate the efflux of Aβ40 or Aβ42 through the blood-brain barrier.[43] Taken together, the following AD-ApoE scenario emerges: ApoE is secreted by astrocytes, forms high-affinity extracellular complexes with Aβ&0x44, and facilitates the proteolytic degradation and/or efflux of Aβ from the AD brain.

This model suggests that increased ApoE secretion from astrocytes will enhance Aβ clearance from the brain, reduce plaque burden, and lead to enhanced cognitive behavior. Significantly, orally available LXR agonists increase ApoE expression, reduce hippocampal Aβ levels, and improve contextual memory in Tg2576 mice.[42,44] Although the adverse effects of LXR agonists, increased plasma lipids and hepatic steatosis,[26,45] limit the utility of this class of molecules, these studies provide an important proof of concept for the potential clinical importance of compounds that increase astrocytic ApoE secretion by non-LXR mechanisms.

The human astrocytoma cell line CCF-STTG1 constitutively secretes ApoE and forms lipoprotein complexes.[25] Secretion of ApoE is increased by addition of cholesterol:phospholipid liposomes[25] and LXR agonists (**Fig. 2**),[27] well-known modulators of ApoE secretion in nonneuronal cell lines. Development of enzyme-linked immunosorbent assays to measure ApoE secretion[46] provides the basis of a screening assay (**Fig. 2**), but to our knowledge, this is the first description of a statistically validated, MTS-ready ApoE secretion assay. Molecules of interest will increase ApoE secretion by a non-LXR mechanism.

Osteoporosis: Wnt pathway

Activation of the canonical Wnt pathway through β-catenin is critical for normal bone development.[7] As reviewed by Krishnan et al.,[8] multiple mutations in the Wnt pathway have been shown to modulate bone formation. In humans and mice, loss-of-function and gain-of-function mutations in the Wnt co-receptor, LRP5, are associated with low bone mineral density skeletal fragility and increased bone density, respectively. In addition, expression of dickkopf (DKK1) and sclerostin (SOST), naturally occurring negative regulators of LRP5 that disrupt the Wnt signaling pathway, are associated with loss of bone mass. Transgenic mice expressing constitutively active β-catenin have increased bone mass and rescue the loss of bone phenotype in LRP5-null mice, indicating the importance of the canonical Wnt signaling pathway in the mechanism of bone formation.[47] Taken together, these findings provide strong validation for activating the canonical Wnt pathway for antiosteoporosis drug discovery.[8,47]

The Wnt signaling pathway is complex, and multiple approaches have been taken to identify small-molecule activators.[48] Approaches include neutralization of inhibitors such as soluble frizzled related protein-1, DKK-1, and SOST and inhibition of GSK3-β. Compound screens have been conducted to identify modulators of the Wnt pathway with the LEF/TCF–driven luciferase reporter in a transfected HEK 293 cell line[49] and through high-content screening in primary human cells.[50,51] Use of transfected cell lines may limit the ability to identify physiologically relevant modulators of the Wnt pathway due to differences in cellular context and expression levels of relevant components. In this respect, screens using preosteoblast-like cells may have a greater potential to identify compounds that are active in bone cells.

In this study, C2C12 cells, a murine cell line with multilineage potential,[52,53] and an intact Wnt pathway that is modulated by DKK1,[54] SOST,[55] and GSK3-β[56] were used to identify potentiators/agonists of the canonical Wnt signaling pathway that enhance formation of an osteoblast-like phenotype as measured by an increase in cellular ALP activity. Compounds of interest will induce β-catenin nuclear translocation and increase cellular ALP activity with similar potencies (**Fig. 6E**).

Oncology: angiogenesis

Neovascularization is a complex process that requires the migration, differentiation, physical interaction, and coordinated cellular signaling of precursor and mature forms of endothelial cells with stromal cells (fibroblasts, pericytes, and smooth muscle). VEGF is recognized as the dominant proangiogenic factor, but other factors such as fibroblast growth factor, epidermal growth factor, hepatocyte growth factor, angiopoietins, thrombomodulin, notch ligands, and transforming growth factor-β can promote, inhibit, or modulate angiogenesis (see Folkman[12] and Adams and Alitalo[14] for reviews).

It is difficult to adequately model a complex biology such as angiogenesis as an in vitro system. Terminally differentiated endothelial cells form tubelike structures when grown on matrigel, an extracellular matrix extract (see Arnaoutova et al.[57] for review), which contains somewhat variable amounts of various growth factors.[58] Although this assay has been used successfully for 20 years, the physical properties of the extract and the variable thickness of the resulting three-dimensional matrix make the use of automated liquid handling and automated imaging, techniques essential for enablement of a reproducible, high-capacity assay, problematic.

Alternatively, feeder layers of fibroblasts[59] or smooth muscle cells[60] have been used as a matrix for angiogenesis assays using differentiated endothelial cells. These assay systems provide a stroma-like microenvironment and are compatible with automated liquid handling and microscopy; however, the limited passage potential of primary cells imposes practical restrictions on the amount of cells available for testing and potentially adds assay variability, factors that limit assay capacity and statistical robustness.

Recently, progenitor cells of endothelial and stromal cells have been shown to form functional blood vessels in vivo when co-cultured in a collagen-fibrin matrix surgically implanted into immunodeficient mice.[61] This study used ECFCs, the "true" endothelial precursor cell population that likely originates from the vasculature but are distinct from marrow-derived endothelial accessory cells (typically referred to as EPCs), which stimulate angiogenesis but do not physically incorporate into a vascular structure.[62] The stromal precursor cells used by Traktuev et al.[61] were mesenchymal-like adipose-derived stem cells, a cell type that has pericyte-like properties,[63,64] greatly enhance tube formation of ECFCs,[61] and can be induced to differentiate into adipose, osteoblast, and chondrocyte lineages (see Gimble et al.[65] for review). Similar mesenchymal-like stem cells have been isolated from the perivascular regions of several adult tissues, suggesting that pericyte-like cells may represent a general multipotent stem cell population located in a perivascular niche.[66]

Significantly, ADSCs take a periendothelial position and express the pericyte marker smooth muscle actin when co-cultured with ECFCs under conditions that lead to functional vessel formation in vivo.[61] These findings suggest that co-culture of ECFCs and ADSCs may better mimic the interplay of signaling pathways, cell-cell interactions, and diverse cellular functions that occur during neovascularization. In addition, the rapid formation of the tube network observed with ECFC-ADSC co-culture (**Fig. S2**) provides a tactical advantage to the slower co-culture systems using Huvec cells with fibroblast or smooth muscle cell feeder layers.[59,60] Compounds of interest will inhibit angiogenesis by novel mechanisms that are distinct from current VEGF pathway–directed agents.

Oncology: G2/M arrest

Cell division is a fundamental process for all organisms and has been a rich historical source for identifying compounds useful in treating cancer. High-content cell cycle assays have been used to identify compounds with novel mechanisms of action,[3] novel compounds for established cell cycle targets,[67,68] and genome-scale RNAi profiling.[69]

The PD^2 cell cycle assay provides a statistically robust and high-throughput means for the general scientific community to test their novel compounds in a multiplexed cell-based assay measuring DNA content, DNA condensation, and cellular levels of cyclin B and pH3 (**Fig. 5**). Compounds of interest inhibit cell cycle in a G2 or M phase, are antiproliferative, and do not work via tubulin polymerization/depolymerization and known cell cycle kinases.

Concluding remarks

The productivity crisis that the pharmaceutical industry faces is important with regard to the economics of the industry, but more importantly, it impedes progress on improving humanity's quality of life. Undoubtedly, there are many aspects to this very complex and multifaceted problem, but innovation in drug discovery and target validation is an area that is likely to be key.[70] Toward this end, open innovation models that promote collaboration between academic and industrial research groups provide a mechanism in which resources and expertise can be shared between these traditionally distinct cultures.[71,72] In this communication, we have summarized the initial assays associated with and the early compound testing results from the PD^2 Initiative. PD^2 has provided access to novel chemical diversity that is <85% similar to known drugs and compounds registered in the Lilly collection. The results presented here indicate that much of this novel chemical diversity is biologically relevant, as demonstrated by good potency in and selectivity between various phenotypic assay modules (**Fig. 6**). Significantly, the low degree of structural similarity between PD^2 molecules and known drugs and the Lilly compound collection suggests that molecules tested in PD^2 are likely to have molecular mechanisms distinct from previously available chemical diversity.[35]

These observations lead to a thought-provoking, albeit speculative, notion. Recent analyses of marketed drugs indicate that they interact with between 266[73] and 394[74] molecular target proteins encoded by the human genome. Based on sequence homology extrapolations of the confirmed drug targets known in 2005, the "druggable genome" was estimated to be composed of roughly 1100 molecular targets,[73] a figure that is less than 4% of the proteins estimated to be encoded by the human genome.[75] In light of the observed prevalence of confirmed biological activity from the novel chemical diversity sampled by PD^2 thus far (**Fig. 6**), one might question whether the druggable genome[74] represents the sum of the molecular targets amenable to manual chemical modulation or merely reflects the limited number of molecular targets that humankind has thus far exploited through drug discovery. Although it is premature to speculate on the outcome and long-term impact of PDD approaches and the PD^2 Initiative, we believe that current drugs represent only the tip of the iceberg with regard to potential therapeutic mechanisms and pharmacologically relevant molecular targets. Chemical diversity is large and biology complex; lead generation strategies that directly interrogate therapeutically relevant biology and are agnostic to the molecular target/signaling pathway may provide a means for the pharmaceutical industry to implement an innovative drug discovery strategy that mitigates the risk associated with target validation. Only time in conjunction with appropriate risk taking will provide information as to whether PDD approaches will be an asset or hindrance to drug discovery in the post-genomic world.

ACKNOWLEDGMENTS

The authors acknowledge Joyce Boadt, Pierre-Alexandre Brault, William Chin, Jeffery Dage, Thomas Engler, Maria Alvim-Gaston, David Gwaltney, Horst Hemmerle, Richard Higgs, Aidas Kriauciunas, Julie Moyers, Vaibhav Narayan, Marta Piñeiro-Nuñez, Daniel H. Robertson, Anja Stauber, Sharon Semones, Larry Stramm, and Ian Watson for their support of PD^2. The authors also acknowledge Louis Stancato, Mark Uhlik, Steven Paul, Ronald Demattos, Rebecca Owens, and Alexander Efanov for their helpful discussions regarding the phenotypic assays.

REFERENCES

1. Lee, J. A.; Cox, K.; Kriauciunas, A.; Chu, S. The Roles of High Content Cellular Imaging in Lead Optimization. In *High Content Screening: Science, Techniques, and Applications*; Haney, S Ed. John Wiley and Sons: New York, **2008**; 249–268.
2. Low, J.; Stancato, L.; Lee, J.; Sutherland, J. J. Prioritizing Hits from Phenotypic High-Content Screens. *Curr. Opin. Drug. Discov. Dev*. **2008**, *11*, 338–345.
3. Mayer, T. U.; Kapoor, T. M.; Haggarty, S. J.; King, R. W.; Schreiber, S. L.; Mitchison, T. J. Small Molecule Inhibitor of Mitotic Spindle Bipolarity Identified in a Phenotype-Based Screen. *Science*. **1999**, *286*, 971–974.
4. Yarrow, J. C.; Totsukawa, G.; Charras, G. T.; Mitchison, T. J. Screening for Cell Migration Inhibitors via Automated Microscopy Reveals a Rho-Kinase Inhibitor. *Chem. Biol*. **2005**, *12*, 385–395.
5. Chen, S.; Do, J. T.; Zhang, Q.; Yao, S.; Yan, F.; Peters, E. C.; Scholer, H. R.; Schultz, P. G.; Ding, S. Self-Renewal of Embryonic Stem Cells by a Small Molecule. *Proc. Natl. Acad. Sci. U. S. A*. **2006**, *103*, 17266–17271.
6. Davis, S.; Granner, D. Insulin, Oral Hypoglycemic Agents, and the Pharmacology of the Endocrine Pancreas. In *Goodman and Gilman's the Pharmacological Basis of Therapeutics*. McGraw-Hill: New York, **2001**; 1679–1714.
7. Cadigan, K. M.; Nusse, R. Wnt Signaling: A Common Theme in Animal Development. *Genes Dev*. **1997**, *11*, 3286–3305.
8. Krishnan, V.; Bryant, H. U.; Macdougald, O. A. Regulation of Bone Mass by Wnt Signaling. *J. Clin. Invest*. **2006**, *116*, 1202–1209.
9. Strittmatter, W. J.; Saunders, A. M.; Schmechel, D.; Pericak-Vance, M.; Enghild, J.; Salvesen, G. S.; Roses, A. D. Apolipoprotein E: High-Avidity Binding to Beta-Amyloid and Increased Frequency of Type 4 Allele in Late-Onset Familial Alzheimer Disease. *Proc. Natl. Acad. Sci. U. S. A*. **1993**, *90*, 1977–1981.
10. Corder, E. H.; Saunders, A. M.; Strittmatter, W. J.; Schmechel, D. E.; Gaskell, P. C.; Small, G. W.; Roses, A. D.; Haines, J. L.; Pericak-Vance, M. A. Gene Dose of Apolipoprotein E Type 4 Allele and the Risk of Alzheimer's Disease in Late Onset Families. *Science*. **1993**, *261*, 921–923.
11. Chabner, B. A.; Allegra C. J.; Curt, G. A.; Calabresi, P.: Antineoplastic Agents. In *Goodman and Gilman's The Pharmacological Basis of Therapeutics*. McGraw-Hill: New York, **1996**; 1233–1287.
12. Folkman, J.: Angiogenesis: An Organizing Principle for Drug Discovery? *Nat. Rev. Drug Discov*. **2007**, *6*, 273–286.
13. Atkins, M.; Jones, C. A.; Kirkpatrick, P. Sunitinib Maleate. *Nat. Rev. Drug. Discov*. **2006**, *5*, 279–280.

14. Adams, R. H.; Alitalo, K. Molecular Regulation of Angiogenesis and Lymphangiogenesis. *Nat. Rev. Mol. Cell Biol*. **2007**, *8*, 464–478.
15. Willert, K.; Brown, J. D.; Danenberg, E.; Duncan, A. W.; Weissman, I. L.; Reya, T.; Yates, J. R. III; Nusse, R. Wnt Proteins Are Lipid-Modified and Can Act as Stem Cell Growth Factors. *Nature*. **2003**, *423*, 448–452.
16. Iversen, P. W.; Eastwood, B. J.; Sittampalam, G. S.; Cox, K. L. A Comparison of Assay Performance Measures in Screening Assays: Signal Window, Z′ Factor, and Assay Variability Ratio. *J. Biomol. Screen*. **2006**, *11*, 247–252.
17. Zhang, J. H.; Chung, T. D.; Oldenburg, K. R. A Simple Statistical Parameter for Use in Evaluation and Validation of High Throughput Screening Assays. *J. Biomol. Screen*. **1999**, *4*, 67–73.
18. Eastwood, B. J.; Farmen, M. W.; Iversen, P. W.; Craft, T. J.; Smallwood, J. K.; Garbison, K. E.; Delapp, N. W.; Smith, G. F. The Minimum Significant Ratio: A Statistical Parameter to Characterize the Reproducibility of Potency Estimates from Concentration-Response Assays and Estimation by Replicate-Experiment Studies. *J. Biomol. Screen*. **2006**, *11*, 253–261.
19. Asfari, M.; Janjic, D.; Meda, P.; Li, G.; Halban, P. A.; Wollheim, C. B. Establishment of 2-Mercaptoethanol-Dependent Differentiated Insulin-Secreting Cell Lines. *Endocrinology*. **1992**, *130*, 167–178.
20. Matschinsky, F. M. Assessing the Potential of Glucokinase Activators in Diabetes Therapy. *Nat. Rev. Drug Discov*. **2009**, *8*, 399–416.
21. Efanov, A. M.; Barrett, D. G.; Brenner, M. B.; Briggs, S. L.; Delaunois, A.; Durbin, J. D.; Giese, U.; Guo, H.; Radloff, M.; Gil, G. S.; Sewing, S.; Wang, Y.; Weichert, A.; Zaliani, A.; Gromada, J. A Novel Glucokinase Activator Modulates Pancreatic Islet and Hepatocyte Function. *Endocrinology*. **2005**, *146*, 3696–3701.
22. Brenner, M. B.; Gromada, J.; Efanov, A. M.; Bokvist, K.; Mest, H. J. Restoration of First-Phase Insulin Secretion by the Imidazoline Compound LY374284 in Pancreatic Islets of Diabetic db/db Mice. *Ann. N. Y. Acad. Sci*. **2003**, *1009*, 332–340.
23. Efanov, A. M.; Zaitsev, S. V.; Mest, H. J.; Raap, A.; Appelskog, I. B.; Larsson, O.; Berggren, P. O.; Efendic, S. The Novel Imidazoline Compound BL11282 Potentiates Glucose-Induced Insulin Secretion in Pancreatic Beta-Cells in the Absence of Modulation of K(ATP) Channel Activity. *Diabetes*. **2001**, *50*, 797–802.
24. Malaisse, W. J.; Sener, A.; Herchuelz, A.; Carpinelli, A. R.; Poloczek, P.; Winand, J.; Castagna, M. Insulinotropic Effect of the Tumor Promoter 12-O-Tetradecanoylphorbol-13-Acetate in Rat Pancreatic Islets. *Cancer Res*. **1980**, *40*, 3827–3831.
25. Krul, E. S.; Tang, J. Secretion of Apolipoprotein E by an Astrocytoma Cell Line. *J. Neurosci. Res*. **1992**, *32*, 227–238.
26. Schultz, J. R.; Tu, H.; Luk, A.; Repa, J. J.; Medina, J. C.; Li, L.; Schwendner, S.; Wang, S.; Thoolen, M.; Mangelsdorf, D. J.; Lustig, K. D.; Shan, B. Role of LXRs in Control of Lipogenesis. *Genes Dev*. **2000**, *14*, 2831–2838.
27. Liang, Y.; Lin, S.; Beyer, T. P.; Zhang, Y.; Wu, X.; Bales, K. R.; DeMattos, R. B.; May, P. C.; Li, S. D.; Jiang, X. C.; Eacho, P. I.; Cao, G.; Paul, S. M. A Liver X Receptor and Retinoid X Receptor Heterodimer Mediates Apolipoprotein E Expression, Secretion and Cholesterol Homeostasis in Astrocytes. *J. Neurochem*. **2004**, *88*, 623–634.
28. Stein, G. S.; Lian, J. B.; Stein, J. L.; Van Wijnen, A. J.; Montecino, M. Transcriptional Control of Osteoblast Growth and Differentiation. *Physiol. Rev*. **1996**, *76*, 593–629.
29. Engler, T. A.; Henry, J. R.; Malhotra, S.; Cunningham, B.; Furness, K.; Brozinick, J.; Burkholder, T. P.; Clay, M. P.; Clayton, J.; Diefenbacher, C.; Hawkins, E.; Iversen, P. W.; Li, Y.; Lindstrom, T. D.; Marquart, A. L.; McLean, J.; Mendel, D.; Misener, E.; Briere, D.; O'Toole, J. C.; Porter, W. J.; Queener, S.; Reel, J. K.; Owens, R. A.; Brier, R. A.; Eessalu, T. E.; Wagner, J. R.; Campbell, R. M.; Vaughn, R. Substituted 3-imidazo[1,2-a] pyridin-3-yl- 4-(1,2,3,4-tetrahydro-[1,4]diazepino-[6,7,1-hi]indol-7-yl) pyrrole-2,5-dion Is a Highly Selective and Potent Inhibitor of Glycogen Synthase Kinase-3. *J. Med. Chem*. **2004**, *47*, 3934–3937.
30. Barabasz, A.; Foley, B.; Otto, J. C.; Scott, A.; Rice, J. The Use of High-Content Screening for the Discovery and Characterization of Compounds That Modulate Mitotic Index and Cell Cycle Progression by Differing Mechanisms of Action. *Assay Drug. Dev. Technol*. **2006**, *4*, 153–163.
31. Gasparri, F.; Cappella, P.; Galvani, A. Multiparametric Cell Cycle Analysis by Automated Microscopy. *J. Biomol. Screen*. **2006**, *11*, 586–598.
32. Grove, L. E.; Ghosh, R. N. Quantitative Characterization of Mitosis-Blocked Tetraploid Cells Using High Content Analysis. *Assay Drug Dev. Technol*. **2006**, *4*, 421–442.
33. Kerr, J. F.; Wyllie, A. H.; Currie, A. R.; Apoptosis: A Basic Biological Phenomenon with Wide-Ranging Implications in Tissue Kinetics. *Br. J. Cancer*. **1972**, *26*, 239–257.
34. Snyder, J. A.; Hamilton, B. T.; Mullins, J. M. Loss of Mitotic Centrosomal Microtubule Initiation Capacity at the Metaphase-Anaphase Transition. *Eur. J. Cell. Biol*. **1982**, *27*, 191–199.
35. Martin, Y. C.; Kofron, J. L.; Traphagen, L. M. Do Structurally Similar Molecules Have Similar Biological Activity? *J. Med. Chem*. **2002**, *45*, 4350–4358.
36. Zhou, J. R.; Mukherjee, P.; Gugger, E. T.; Tanaka, T.; Blackburn, G. L.; Clinton, S. K. Inhibition of Murine Bladder Tumorigenesis by Soy Isoflavones via Alterations in the Cell Cycle, Apoptosis, and Angiogenesis. *Cancer Res*. **1998**, *58*, 5231–5238.
37. Ahren, B. Islet G Protein-Coupled Receptors as Potential Targets for Treatment of Type 2 Diabetes. *Nat. Rev. Drug Discov*. **2009**, *8*, 369–385.
38. Wu, W.; Shang, J.; Feng, Y.; Thompson, C. M.; Horwitz, S.; Thompson, J. R.; MacIntyre, E. D.; Thornberry, N. A.; Chapman, K.; Zhou, Y. P.; Howard, A. D.; Li, J. Identification of Glucose-Dependant Insulin Secretion Targets in Pancreatic Beta Cells by Combining Defined-Mechanism Compound Library Screening and siRNA Gene Silencing. *J. Biomol. Screen*. **2008**, *13*, 128–134.
39. Roses, A. D. Apolipoprotein E Alleles as Risk Factors in Alzheimer's Disease. *Annu. Rev. Med*. **1996**, *47*, 387–400.
40. Holtzman, D. M.; Fagan, A. M.; Mackey, B.; Tenkova, T.; Sartorius, L.; Paul, S. M.; Bales, K.; Ashe, K. H.; Irizarry, M. C.; Hyman, B. T. Apolipoprotein E Facilitates Neuritic and Cerebrovascular Plaque Formation in an Alzheimer's Disease Model. *Ann. Neurol*. **2000**, *47*, 739–747.
41. Ji, Y.; Gong, Y.; Gan, W.; Beach, T.; Holtzman, D. M.; Wisniewski, T. Apolipoprotein E Isoform-Specific Regulation of Dendritic Spine Morphology in Apolipoprotein E Transgenic Mice and Alzheimer's Disease Patients. *Neuroscience*. **2003**, *122*, 305–315.
42. Jiang, Q.; Lee, C. Y.; Mandrekar, S.; Wilkinson, B.; Cramer, P.; Zelcer, N.; Mann, K.; Lamb, B.; Willson, T. M.; Collins, J. L.; Richardson, J. C.; Smith, J. D.; Comery, T. A.; Riddell, D.; Holtzman, D. M.; Tontonoz, P.; Landreth, G. E. ApoE Promotes the Proteolytic Degradation of Abeta. *Neuron*. **2008**, *58*, 681–693.
43. Deane, R.; Sagare, A.; Hamm, K.; Parisi, M.; Lane, S.; Finn, M. B.; Holtzman, D. M.; Zlokovic, B. V. apoE Isoform-Specific Disruption of Amyloid Beta Peptide Clearance from Mouse Brain. *J. Clin. Invest*. **2008**, *118*, 4002–4013.
44. Riddell, D. R.; Zhou, H.; Comery, T. A.; Kouranova, E.; Lo, C. F.; Warwick, H. K.; Ring, R. H.; Kirksey, Y.; Aschmies, S.; Xu, J.; Kubek, K.; Hirst, W. D.; Gonzales, C.; Chen, Y.; Murphy, E.; Leonard, S.; Vasylyev, D.; Oganesian, A.; Martone, R. L.; Pangalos, M. N.; Reinhart, P. H.; Jacobsen, J. S. The LXR Agonist TO901317 Selectively Lowers Hippocampal Abeta42 and Improves Memory in the Tg2576 Mouse Model of Alzheimer's Disease. *Mol. Cell Neurosci*. **2007**, *34*, 621–628.

45. Grefhorst, A.; Elzinga, B. M.; Voshol, P. J.; Plosch, T.; Kok, T.; Bloks, V. W.; van der Sluijs, F. H.; Havekes, L. M.; Romijn, J. A.; Verkade, H. J.; Kuipers, F. Stimulation of Lipogenesis by Pharmacological Activation of the Liver X Receptor Leads to Production of Large, Triglyceride-Rich Very Low Density Lipoprotein Particles. *J. Biol. Chem*. **2002**, *277*, 34182–34190.
46. Starck, M.; Bertrand, P.; Pepin, S.; Schiele, F.; Siest, G.; Galteau, M. M. Effects of Pro-Inflammatory Cytokines on Apolipoprotein E Secretion by a Human Astrocytoma Cell Line (CCF-STTG1). *Cell Biochem. Funct*. **2000**, *18*, 9–16.
47. Case, N.; Rubin, J. β-catenin—A Supporting Role in the Skeleton. *J. Cell Biochem*. **2010**, *110*, 545–553.
48. Hoeppner, L. H.; Secreto, F. J.; Westendorf, J. J. Wnt Signaling as a Therapeutic Target for Bone Diseases. *Expert Opin. Ther. Targets*. **2009**, *13*, 485–496.
49. Zhang, Q.; Major, M. B.; Takanashi, S.; Camp, N. D.; Nishiya, N.; Peters, E. C.; Ginsberg, M. H.; Jian, X.; Randazzo, P. A.; Schultz, P. G.; Moon, R. T.; Ding, S. Small-Molecule Synergist of the Wnt/Beta-Catenin Signaling Pathway. *Proc. Natl. Acad. Sci. U. S. A*. **2007**, *104*, 7444–7448.
50. Borchert, K. M.; Galvin, R. J.; Frolik, C. A.; Hale, L. V.; Halladay, D. L.; Gonyier, R. J.; Trask, O. J.; Nickischer, D. R.; Houck, K. A. High-Content Screening Assay for Activators of the Wnt/Fzd Pathway in Primary Human Cells. *Assay Drug Dev. Technol*. **2005**, *3*, 133–141.
51. Borchert, K. M.; Sells Galvin, R. J.; Hale, L. V.; Trask, O. J.; Nickischer, D. R.; Houck, K. A. Screening for Activators of the Wingless Type/Frizzled Pathway by Automated Fluorescent Microscopy. *Methods Enzymol*. **2006**, *414*, 140–150.
52. Katagiri, T.; Yamaguchi, A.; Komaki, M.; Abe, E.; Takahashi, N.; Ikeda, T.; Rosen, V.; Wozney, J. M.; Fujisawa-Sehara, A.; Suda, T. Bone Morphogenetic Protein-2 Converts the Differentiation Pathway of C2C12 Myoblasts into the Osteoblast Lineage. *J. Cell. Biol*. **1994**, *127*, 1755–1766.
53. Lee, K. S.; Kim, H. J.; Li, Q. L.; Chi, X. Z.; Ueta, C.; Komori, T.; Wozney, J. M.; Kim, E. G.; Choi, J. Y.; Ryoo, H. M.; Bae, S. C. Runx2 Is a Common Target of Transforming Growth Factor Beta1 and Bone Morphogenetic Protein 2, and Cooperation between Runx2 and Smad5 Induces Osteoblast-Specific Gene Expression in the Pluripotent Mesenchymal Precursor Cell Line C2C12. *Mol. Cell Biol*. **2000**, *20*, 8783–8792.
54. Tian, E.; Zhan, F.; Walker, R.; Rasmussen, E.; Ma, Y.; Barlogie, B.; Shaughnessy, J. D. Jr. The Role of the Wnt-Signaling Antagonist DKK1 in the Development of Osteolytic Lesions in Multiple Myeloma. *N. Engl. J. Med*. **2003**, *349*, 2483–2494.
55. Yang, F.; Tang, W.; So, S.; Crombrugghe, B.; Zhang, C. Sclerostin is a direct target of osteoblast-specific transcription factor osterix. *Biochem. Biophys. Res. Commun*. **2010**, *400*, 684–688.
56. Stewart, J. P.; Shaughnessy, J. D., Jr., . Role of Osteoblast Suppression in Multiple Myeloma. *J. Cell Biochem*. **2006**, *98*, 1–13.
57. Arnaoutova, I.; George, J.; Kleinman, H. K.; Benton, G. The Endothelial Cell Tube Formation Assay on Basement Membrane Turns 20: State of the Science and the Art. *Angiogenesis*. **2009**, *12*, 267–274.
58. Vukicevic, S.; Kleinman, H. K.; Luyten, F. P.; Roberts, A. B.; Roche, N. S.; Reddi, A. H. Identification of Multiple Active Growth Factors in Basement Membrane Matrigel Suggests Caution in Interpretation of Cellular Activity Related to Extracellular Matrix Components. *Exp. Cell Res*. **1992**, *202*, 1–8.
59. Donovan, D.; Brown, N. J.; Bishop, E. T.; Lewis, C. E. Comparison of Three In Vitro Human "Angiogenesis" Assays With Capillaries Formed In Vivo. *Angiogenesis*. **2001**, *4*, 113–121.
60. Evensen, L.; Micklem, D. R.; Blois, A.; Berge, S. V.; Aarsaether, N.; Littlewood-Evans, A.; Wood, J.; Lorens, J. B. Mural Cell Associated VEGF Is Required for Organotypic Vessel Formation. *PLoS. One*. **2009**, *4*, e5798.
61. Traktuev, D. O.; Prater, D. N.; Merfeld-Clauss, S.; Sanjeevaiah, A. R.; Saadatzadeh, M. R.; Murphy, M; Johnstone, B. H.; Ingram, D. A.; March, K. L. Robust Functional Vascular Network Formation In Vivo by Cooperation of Adipose Progenitor and Endothelial Cells. *Circ. Res*. **2009**, *104*, 1410–1420.
62. Yoder, M. C. Is Endothelium the Origin of Endothelial Progenitor Cells? *Arterioscler. Thromb. Vasc. Biology*. **2010**, *30*, 1094–1103.
63. Amos, P. J.; Shang, H.; Bailey, A. M.; Taylor, A.; Katz, A. J.; Peirce, S. M. IFATS Collection: The Role of Human Adipose-Derived Stromal Cells in Inflammatory Microvascular Remodeling and Evidence of a Perivascular Phenotype. *Stem Cells*. **2008**, *26*, 2682–2690.
64. Traktuev, D. O.; Merfeld-Clauss, S.; Li, J.; Kolonin, M.; Arap, W.; Pasqualini, R.; Johnstone, B. H.; March, K. L. A Population of Multipotent CD34-Positive Adipose Stromal Cells Share Pericyte and Mesenchymal Surface Markers, Reside in a Periendothelial Location, and Stabilize Endothelial Networks. *Circ. Res*. **2008**, *102*, 77–85.
65. Gimble, J. M.; Katz, A. J.; Bunnell, B. A. Adipose-Derived Stem Cells for Regenerative Medicine. *Circ. Res*. **2007**, *100*, 1249–1260.
66. Crisan, M.; Yap, S.; Casteilla, L.; Chen, C. W.; Corselli, M.; Park, T. S.; Andriolo, G.; Sun, B.; Zheng, B.; Zhang, L.; Norotte, C.; Teng, P. N.; Traas, J.; Schugar, R.; Deasy, B. M.; Badylak, S.; Buhring, H. J.; Giacobino, J. P.; Lazzari, L.; Huard, J.; Peault, B. A Perivascular Origin for Mesenchymal Stem Cells in Multiple Human Organs. *Cell Stem Cell*. **2008**, *3*, 301–313.
67. Gururaja, T. L.; Goff, D.; Kinoshita, T.; Goldstein, E.; Yung, S.; McLaughlin, J.; Pali, E.; Huang, J.; Singh, R.; Daniel-Issakani, S.; Hitoshi, Y.; Cooper, R. D.; Payan, D. G. R-253 Disrupts Microtubule Networks in Multiple Tumor Cell Lines. *Clin. Cancer Res*. **2006**, *12*, 3831–3842.
68. Wilson, C. J.; Si, Y.; Thompsons, C. M.; Smellie, A.; Ashwell, M. A.; Liu, J. F.; Ye, P.; Yohannes, D.; Ng, S. C. Identification of a Small Molecule that Induces Mitotic Arrest Using a Simplified High-Content Screening Assay and Data Analysis Method. *J. Biomol. Screen*. **2006**, *11*, 21–28.
69. Kittler, R.; Pelletier, L.; Heninger, A. K.; Slabicki, M.; Theis, M.; Miroslaw, L.; Poser, I.; Lawo, S.; Grabner, H.; Kozak, K.; Wagner, J.; Surendranath, V.; Richter, C.; Bowen, W.; Jackson, A. L.; Habermann, B.; Hyman, A. A.; Buchholz, F. Genome-Scale RNAi Profiling of Cell Division in Human Tissue Culture Cells. *Nat. Cell Biol*. **2007**, *9*, 1401–1412.
70. Paul, S. M.; Mytelka, D. S.; Dunwiddie, C. T.; Persinger, C. C.; Munos, B. H.; Lindborg, S. R.; Schacht, A. L. How to Improve R&D Productivity: The Pharmaceutical Industry's Grand Challenge. *Nat. Rev. Drug Discov*. **2010**, *9*, 203–214.
71. Hunter, J.; Stephens, S. Is Open Innovation the Way Forward for Big Pharma? *Nat. Rev. Drug. Discov*. **2010**, *9*, 87–88.
72. Munos, B. Can Open-Source Drug R&D Repower Pharmaceutical Innovation? *Clin. Pharmacol. Ther*. **2010**, *87*, 534–536.
73. Overington, J. P.; Al-Lazikani, B.; Hopkins, A. L. How Many Drug Targets Are There? *Nat. Rev. Drug Discov*. **2006**, *5*, 993–996.
74. Yildirim, M. A.; Goh, K. I.; Cusick, M. E.; Barabasi, A. L.; Vidal, M. Drug-Target Network. *Nat. Biotechnol*. **2007**, *25*, 1119–1126.
75. International Human Genome Sequencing Consortium: Finishing the Euchromatic Sequence of the Human Genome. *Nature*. **2004**, *431*, 931–945.

Address correspondence to:
Jonathan A. Lee
Lilly Corporate Center
Drop Code 0703
Indianapolis, IN 46285

E-mail: jonathan_a_lee@lilly.com